Athens Journal of Technology and Engineering - Volume 11, Issue 1,
March 2024 – Pages 9-28

Study on the Stresses Released in a Notched, Postensioned Concrete Beam

By Juan A. Mateu-Sánchez[*], Ester Giménez-Carbó[±], Pedro Serna[°], Carmen Castro-Bugallo[•], Juan Navarro-Gregori[♦] & Jose R. Martí-Vargas[♥]

Structural prestressed concrete elements (SPCE) face uncertainties in accurately assessing the actual prestressing force. Over time, the initial prestressing force decreases due to several factors. Incorrect estimation of prestress losses can lead to design inefficiencies or structural issues. Monitoring the prestressing force can be achieved through instrumentation during casting, but existing SPCE lack such devices, necessitating indirect methods to determine prestressing force variations. This study focuses on analyzing stresses released in a notched post-tensioned concrete beam using the saw-cutting technique. Surface notches induce local decompression, allowing for strain measurements in the isolated concrete block. These measurements, considering uncertainties in initial prestress and material properties, are analyzed through backward calculations. The findings enhance understanding of saw-cutting and enable future applications to determine effective prestressing force in unmonitored SPCE. Further experimental studies are required to explore prestressing force consistency under monitored conditions. This research provides valuable insights into the potential of the saw-cutting technique as a non-destructive testing method for assessing prestressing force in unmonitored SPCE. Accurately determining the prestressing force is crucial for evaluating existing SPCE and ensuring their structural integrity.

Keywords: *prestressed concrete, beam, test, saw-cut, notch*

Introduction

Much of the existing bridges in Europe and the United States, made of structural prestressed concrete elements (SPCE), date back to the 1950s and 1960s and are approaching the end of their service life, regardless of the prestressing technique used (post-tensioning or pretensioning) (FIB 2016). This raises concerns about the condition of these elements and how they affect the overall behavior of the structure. Most SPCE that are nearing the end of their service life were built using outdated codes and regulations that did not consider the deferred effects of

[*]PhD Student, Universitat Politècnica de València, Spain.
[±]Associate Professor, Universitat Politècnica de València, Spain.
[°]Professor, Universitat Politècnica de València, Spain.
[•]Associate Professor, Universitat Politècnica de València, Spain.
[♦]Associate Professor, Universitat Politècnica de València, Spain.
[♥]Professor, Universitat Politècnica de València, Spain.

https://doi.org/10.30958/ajte.11-1-1 doi=10.30958/ajte.11-1-1

concrete and steel with the same importance as they are considered today. The lack of consideration for the magnitude of deferred effects and consequently the state of stress in the structure, combined with the different loading conditions than those anticipated in the design, as well as premature degradation of SPCE, result in a state of stress uncertainty that needs to be addressed immediately.

In the case of prestressed concrete using prestressed steel reinforcement, specifically in post-tensioned concrete elements, the prestressing force experiences a decrease over time due to factors that occur instantaneously and others that are time-dependent. Instantaneous factors include prestress losses caused by friction between steel and concrete, elastic shrinkage of concrete, and loss of fit in the anchorage device. On the other hand, time-dependent factors include creep and shrinkage of concrete, as well as relaxation of the reinforcement steel.

As a result, the peculiarity of prestressed concrete structures becomes highly relevant, as their behavior in terms of tension and deformation depends not only on external loads but especially on the interaction between concrete and active steel that generates prestress. According to Professor Calavera, prestress losses over time represent a complex phenomenon in which the reinforcement is anchored in fluid concrete subjected to progressively decreasing tension (Calavera 2018). Professor Nawy, on the other hand, maintains that it is impossible to accurately determine the magnitude of these losses, especially time-dependent ones, due to the multiplicity of interrelated factors. Different practice codes use empirical methods to estimate such losses, but there are variations among them (Nawy 2005).

For this reason, there is a need to determine the level of prestress acting on the structure to assess the condition of a SPCE, as the influence of prestress on these types of structures is essential and needs to be evaluated to prevent premature aging, excessive deflections, and the occurrence of unexpected cracks. The design of such elements is truly complex since the designer must determine the prestress and estimate the prestress loss so that the structure meets its required performance during its service life, which is particularly challenging when considering deferred effects whose influence has been proven to be significant in the long-term durability of the structure.

Traditionally, periodic visual inspection practices dominate maintenance programs worldwide (Li et al. 2016). However, it is true that these visual inspections are insufficient to meet the current maintenance needs, especially in prestressed concrete structures where damage can often remain hidden due to the compressive effect caused by prestress (Kim et al. 2011, Lynch 2007). Due to the cases of premature aging in SPCE, there is a need to explore new techniques to determine the acting prestress in the structure, aiming to verify if indirect estimation techniques, based on displacements, can predict the prestress force.

Recent studies (Azizinamini et al. 1996, Halsey and Miller 1996), conducted on existing prestressed concrete elements have reported difficulties in determining prestress losses and residual prestress force. Many PCMs were built without proper instrumentation, making it challenging to directly estimate the residual prestress force. In such cases, additional complex factors need to be considered, such as initial prestress, material properties and their evolution, as well as short-

term and long-term prestress losses. These difficulties are associated with assumptions about the characteristics of the prestressing system, time-dependent phenomena, and potential degradation processes. In some instances, uncertainties related to prestressing have led to the collapse of prestressed concrete bridges.

Therefore, according to the Strategic Plan 2020-2023 of the World Road Association - PIARC (2020), it is necessary to promote the use of scientific methods and state of the art techniques in the evaluation of existing structures. This is crucial to address the uncertainties associated with prestressing and ensure the safety and reliability of prestressed concrete structures in service.

In this paper, a study and application of the saw-cut technique for a prestressed concrete beam under controlled laboratory conditions are proposed, in which the results will be analyzed and verified using a finite element model.

To achieve this, the following methodology is proposed, which will present different techniques for obtaining prestress, the selection and justification of the technique used in this study, the properties of both the materials and the beam geometry will be discussed, as well as the instrumentation selected for measurement, arrangement, and the results obtained in the test will be discussed.

Techniques for Obtaining Residual Prestress

The techniques that can be used to obtain residual prestress in prestressed concrete elements (SPCEs) can be divided into two main groups. The first group is called direct methods, which involve continuous monitoring techniques through the inclusion of measurement sensors during the execution of SPCEs.

Within the direct methods, there are two main categories based on the actions on the prestressing tendon. The first category involves measuring the tension in the tendon using techniques such as strain gauges or fiber optic sensors. The second category involves sensors that provide the prestressing force, such as force transducers, electromagnetic sensors, ultrasonics, and others.

Another classification can be made based on measurements on the concrete itself. In this case, displacement measurements on the concrete are used to obtain internal stress-displacement relationships. Techniques such as vibrating wire strain gauges (VWDG) and vibrating beam strain gauges (VBSG) are used for this purpose. Surface displacement measurements can also be obtained using devices in contact with the concrete surface, such as strain gauges or mechanical measurement techniques at localized points. Non-contact techniques like photogrammetry, interferometric laser, scanner, or stripes.

All the above mentioned techniques do not affect SPCEs. However, unfortunately, continuous monitoring sensors are relatively recent techniques and SPCEs nearing the end of their service life, which require more information about their stress state, may not have these continuous monitoring devices available.

There are numerous methods available to obtain the stress state of older structures where information about the evolution of prestress is lacking. These indirect measurement techniques have been developed over time through real-

scale testing. They can be classified based on their impact on the structure into two main groups: destructive and non-destructive methods.

Destructive methods are the most studied and commonly used in practice, especially for structures that have been dismantled and will not be put back into service. Non-destructive methods, on the other hand, are more specific and offer great potential for evaluating SPCEs in service. They are less destructive techniques for obtaining the stress state.

Figure 1. *Scheme Flexural Crack*

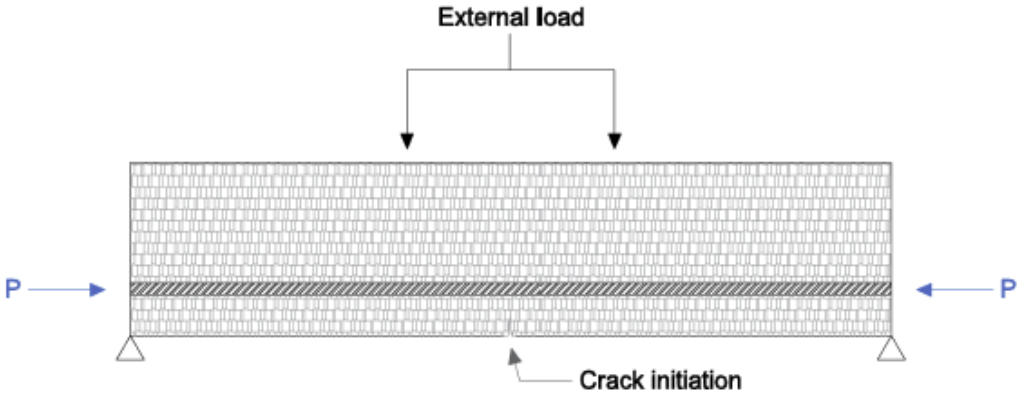

The following are the different indirect methods, both destructive and non-destructive, which demonstrate the testing scheme of each method. One type of method is the Loading Test, which has two main variants based on different applied stress states in the beam. In the first variant, as shown in Figure 1, an SPCE is subjected to a bending moment in a frame where the main objective is to apply a load that generates only normal stresses in the concrete. The load is increased until the first crack appears, resulting in a zero stress on the bottom surface of the beam. Using stress-strain relationships, the applied flexural force can be used to determine the prestressing force acting on the beam. This method has been widely used over time, resulting in a wide range of results. However, its main drawback is the need for laboratory testing and the significant damage inflicted on the beam, including decompression and the formation of cracks that can lead to corrosion and degradation of the steel if the SPCE is put back into service, making it impractical for inspection (Azizinamini et al. 1996, Halsey and Miller 1996, Riessauw and Taerwe 1980, Tabatabai and Dickson 1993, Pessiki et al. 1996, Labia et al. 1997, Naito et al. 2008, Osborn et al. 2012, Pape and Melchers 2013, Botte et al. 2021, Yuan et al. 2015).

Figure 2. *Scheme Crack Re-openning*

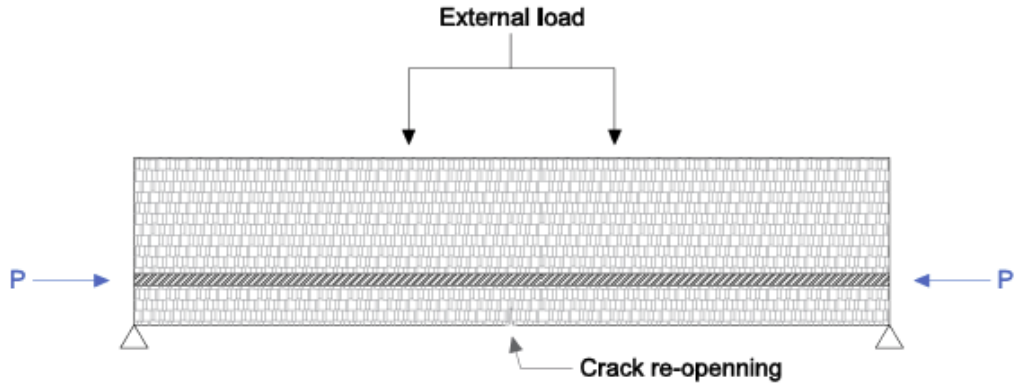

Figure 2 illustrates a method based on the same methodology as the previously discussed technique. In this technique, an applied force causes crack opening, and successive load increments induce the opening of the crack. The crack closure capacity is then analyzed, hence its name crack reopening. This method starts from an initially pre-cracked state. For a long time, this method has been used to analyze beams that have been taken out of service to examine their actual condition and observe the residual prestress in SPCEs.

Figure 3. *Scheme Tendon Cutting*

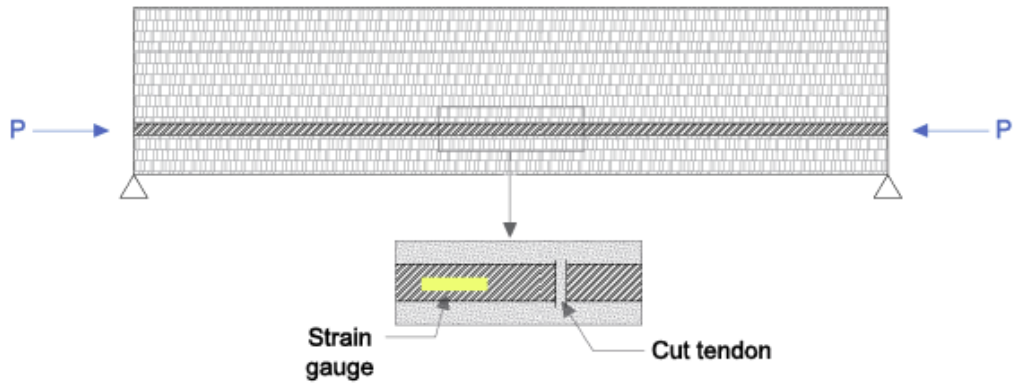

As for the method applied directly to the prestressing cable, two methods are found. The first one is the strand cutting method, where a complete cut is made in the prestressing tendon to observe the deformation released after the cut. Instrumentation is done by placing a strain gauge on the steel, followed by a total cut of the prestressing tendon, as shown in Figure 3. The main drawback of this method is the need to excavate the area around the cable to install the strain gauge, and it renders the SPCE completely unusable as the effect of prestressing is eliminated. This technique has not been extensively used due to the significant number of disadvantages it presents.

Figure 4. *Scheme Strand Tendon*

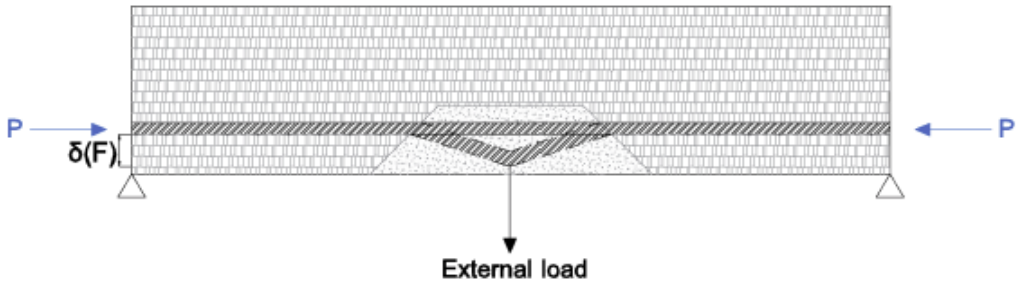

Another technique based on direct actions on the steel is the exposed tendon method. It follows a similar procedure to the previous method, but instead of cutting the tendon, a force is applied perpendicular to the cable. The tension state can be determined based on the displacement that occurs in the cable. It is not clear whether this technique can be considered non-destructive since accessing the prestressing tendon requires removing a significant volume of concrete, which can affect the functional capacity of the beam, as shown in Figure 4.

Lastly, regarding the different techniques for determining residual prestress in SPCEs, techniques based on actions in the concrete stand out. These techniques have been the most widely used in recent years, but there is still a considerable level of uncertainty and parameters that have not been fully controlled yet.

Figure 5. *Scheme Hole/Core Drilling*

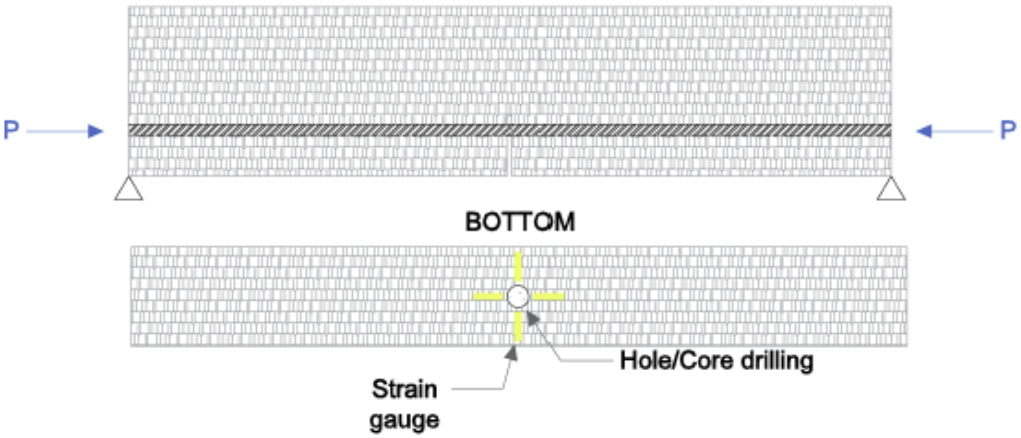

One notable technique is the Hole/Core-Drilling technique, which involves drilling a hole in the concrete using either a drill bit or a core bit, depending on the diameter. It is a simple technique with a straightforward application for measurement. However, according to different studies, it presents high uncertainties due to the unclear path of forces, resulting in significant uncertainty (Kesavan et al. 2005, Parivallal et al. 2011). Figure 5 shows a possible arrangement for performing this reverse measurement technique of the prestressing force using

strain gauges. It is a technique that can be easily restored, allowing the element to be put back into service after minor repairs.

Figure 6. *Scheme Saw-Cut*

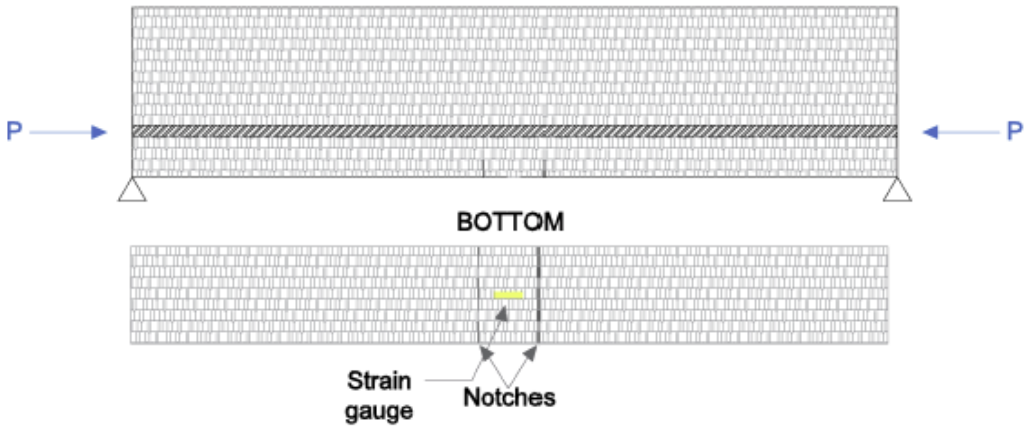

Finally, a technique that has emerged in recent years is the saw-cutting method, which involves creating notches in the concrete. This technique primarily isolates a block of concrete by making cuts in the concrete. This isolation allows measurements of deformations without the interference of prestressing. Various studies (Kralovanec et al. 2021, 2022a, b) demonstrate that by placing a strain gauge in the middle of the isolated block, it is possible to measure the deformation as the notch depth increases. This arrangement can be seen in Figure 6. Therefore, considering the aforementioned information, the apparent conceptual simplicity of the Isolated Concrete Block Method or saw-cutting method (ICBM), along with its low impact on the structure (the cuts only affect the concrete layer and can be resealed) (Bauset-Tortonda et al. 2023), instill confidence in overcoming the limitations associated with the hole-drilling technique (low stress release, instrumentation difficulty, etc.). Thus, the ICBM has clear potential to become a practical, economical, and reliable non-destructive method for assessing SPCEs.

Methodology

Geometry

The experimental specimen is a prestressed concrete element with a total length of 3.20 meters. The free length between supports is 3 meters, which means there is a 20 centimeter space at each end that is not subject to support restrictions. This configuration allows for the analysis of the element's behavior under specific loading and deformation conditions. Regarding the height at which the prestressing cable is placed, it has a straight path and an eccentricity of 0.035 meters with respect to the center of gravity of the concrete gross section.

Figure 7. *Cross Section*

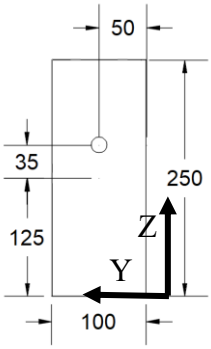

The cross-sectional shape of the specimen has a depth of 0.25 meters and a width of 0.10 meters (see Figure 7). This rectangular cross-section provides an adequate contact surface for prestressing and ensures the strength and stability of the element. Additionally, the size of the cross-section is designed to meet specific design requirements and ensure a sufficient stress concentration capacity due to prestressing to eliminate the Splitting effect. To achieve this, steel distribution plates with a depth of 0.25 meters and a width of 0.10 meters are used. These plates are placed at the ends to efficiently distribute and transmit the prestressing forces. The use of steel distribution plates allows for the application of a uniform and controlled prestressing force to the element. Figure 8 shows the characteristics of the cross-section, as well as the longitudinal view.

Figure 8. *Top and Front View*

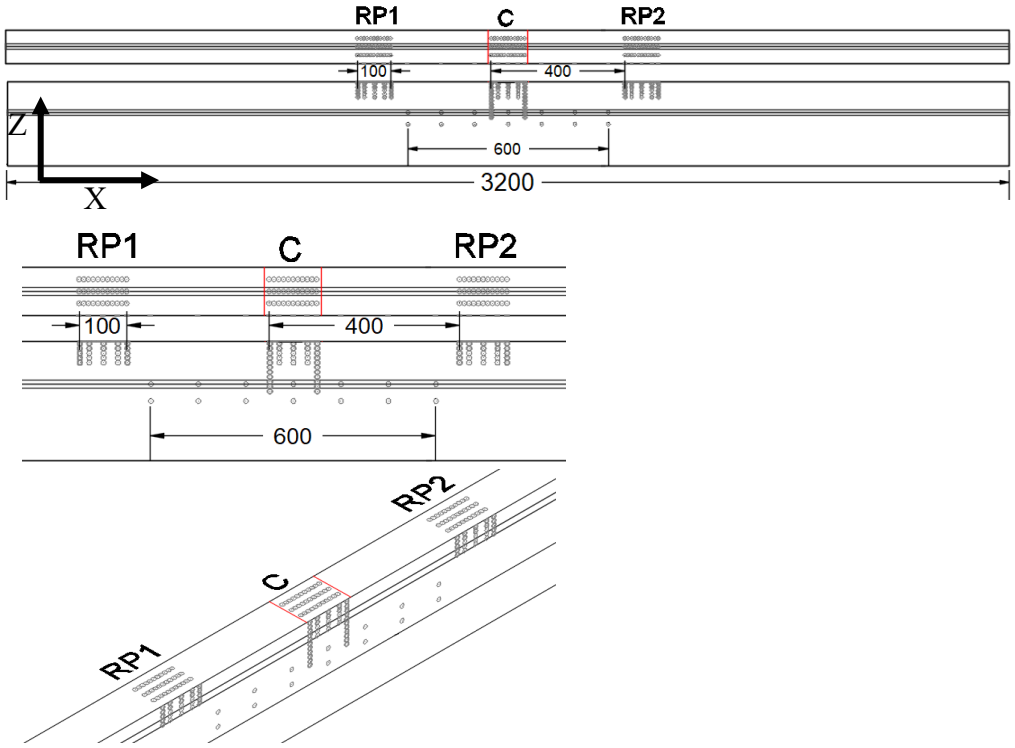

The experimental specimen has been designed and constructed for testing the isolated block method and conducting a detailed analysis of its structural behavior after the notches are made.

Prototype Execution

For the execution of the prototype, metal formwork panels were used, placed on a flat and leveled surface. The formwork panel measured ninety centimeters in width and three meters in length. To achieve a total length of 3.20 meters, an additional formwork panel was placed at a 90-degree angle, resulting in a total formwork length of 3.90 meters, allowing for the production of 3.20-meter beams.

During the execution of the shown beam, the formwork was also used to create two additional constituent beams using the same material. For this purpose, wooden beams were placed along the entire length of the beam, and two cross beams were used to ensure the horizontal alignment of the cable duct. To achieve this, three corrugated steel bars were inserted inside the ducts to ensure parallelism with the longitudinal faces. Alongside the beams, 14 cylindrical control specimens were used to monitor the material properties, compacting them in thirds using 25 blows, as stated in the EC2 standard for concrete control and execution. Figure 9 shows the procedure and pouring of the control specimens.

Figure 9. *Specimen Running Process*

Materials

The concrete used for the execution of the SPCEs in question had certain necessary characteristics to achieve a minimum strength of 27 MPa at 48 hours to allow for transportation and avoid cracking issues. The dosages employed are shown in Tables 1 and 2.

Table 1. *Dosage for Concrete*

Material	**Weight (kg/m^3)**
Gravel 8/16	690 kg
Gravel 4/8	290 kg
Red Sand	820 kg
White Sand	74 kg
Cement	450 kg
Water	180 kg
Additive	6 kg

Table 2. *Material Properties*

Material	Aparent density (kg/m^3)	Dry density (kg/m^3)	Sat density (kg/m^3)
Gravel 8/16	2.76	2.69	2.71
Gravel 4/8	2.76	2.69	2.71
Red Sand	2.74	2.67	2.69
White Sand	2.52	2.46	2.48

Regarding the cement used, it is a type CEM I 42.5 R-SR5 suitable for protection in marine environments, high-strength concrete, and sulfate resistance.

Figure 10. *Abrams Cone and Placement in the Concrete Formwork*

Regarding the manufactured concrete, a fluid concrete was obtained during its execution, corresponding to an Abrams cone value of 25 cm, as shown in Figure 10. Additionally, this fluid concrete facilitated its placement and filling in the formwork, resulting in a more homogeneous surface that will facilitate the instrumentation.

Instrumentation

For the instrumentation of the beam, an effective and user-friendly mechanical method called DEMEC was chosen.

DEMEC (Demountable Mechanical Strain Gauge) is a useful tool that offers several advantages compared to surface-mounted electrical resistance strain gauges for concrete. Here are some reasons why DEMEC is a preferred option:

Precision and reliability: DEMEC allows for precise and reliable deformation measurements. With precision manufacturing and careful use, high measurement accuracy can be achieved at different points of a structure. This is especially important in civil engineering and construction applications where accuracy is crucial for assessing structural integrity and safety.

Cost-effectiveness: DEMEC provides a cost-effective alternative to electrical strain gauges. It does not require complex electrical equipment or complicated installation. Moreover, being a reusable instrument, it can be used for multiple measurements, reducing long-term costs.

Ease of use: DEMEC is user-friendly and does not require specialized technical knowledge. With proper practice, quick and accurate measurements can be made. Additionally, the instrument comes with reference and adjustment bars, further facilitating its implementation.

Adaptability to different materials and structures: Unlike electrical strain gauges that primarily focus on the concrete surface, DEMEC can be used on a wide range of materials and structures. Whether it is concrete, steel, or other structural materials, DEMEC can be adapted to different applications and environments.

Elimination of thermal effects: DEMEC is designed with thermal effects in mind. It uses an Invar reference bar, a metal with a very low coefficient of thermal expansion, which helps eliminate the effects of temperature changes on measurements. Furthermore, if significant temperature changes are expected in the concrete during testing, a simulated concrete bar can be used to eliminate thermal effects on the instrument.

After conducting previous prototypes prior to this specimen, a comparison was made between strain gauges that measure deformation through electrical resistance and mechanical strain gauges. It was observed that the mechanical strain gauges exhibit lower sensitivity to thermal variation compared to the electrical resistance ones. When radial cuts were made near the strain gauge location, the measurements of the mechanical strain gauges were affected due to the temperature increase during the cutting process. These factors have been addressed in other research works (Kralovanec et al. 2021), which discuss potential issues related to temperature variations during sawing and their impact on measurements. Finally, Figure 11 shows the instrumentation plans, with the RP1 zone indicating the beam's center.

The measurement instruments used for the test were a DEMEC device with a 100mm arm and another DEMEC device with a 400mm arm. By using these devices, measurements could be taken from a location far enough from the cutting zones to avoid interference or displacements that could affect the measurements.

Figure 11. *Instrumentation Layout*

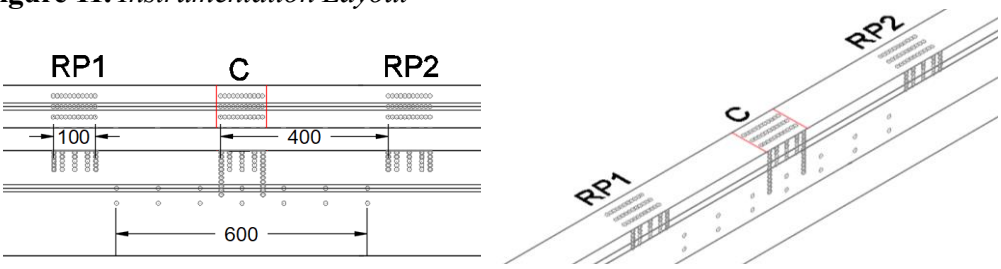

A total of 200 DEMECs were installed. On the top face, three rows of DEMECs were placed at one-centimeter intervals, positioned at heights of Y=25 mm, Y= 50mm, and Y=75mm from the top face. The same arrangement was made for RP1, located at 400mm, and for C, equidistant in the opposite direction from RP2, also at 400mm from RP1. These DEMECs were responsible for measuring the deformation on the top face.

Regarding the lateral faces of the beam, four measurement zones were established. One zone was located at the chord corresponding to the center of gravity of the beam's cross-section (Z=125mm), with 7 DEMECs placed 100mm apart from each other, providing a total control length of 600mm in that zone.

Similarly, another zone was placed at the cable height (Z=160mm), creating two measurement zones to monitor deformation at the beam's central points. Additionally, in order to assess stress concentration once the notches were made at the two cutting points, different measurement points were placed in the central zone to observe displacements at the notch edge as the distance to the cut increased.

Materials Properties

The concrete used for the previously explained specimen had an average compressive strength of 41.66 MPa at 48 hours, obtained from the rupture of three cylindrical specimens. The modulus of elasticity was determined to be 34,645 MPa. On the test day, which was 7 days after execution, the compressive strength values of the specimens were 51 MPa, 52 MPa, and 53 MPa, while the modulus of elasticity of the concrete at 7 days was determined to be 36,579 MPa.

Regarding the steel used for the active reinforcement, it was Y1860 S7 steel with a diameter of 13mm, and the manufacturer provided a modulus of elasticity of 195,000 MPa.

Materials Used to Measure

The various devices used to perform the test under controlled conditions are discussed below:

Hydraulic jack: The jack used for tensioning corresponded to a mono-strand jack with load regulation through a manual hydraulic circuit, as shown in Figure 12.

Figure 12. *Hydraulic Jack for Prestress*

To measure the forces during tensioning, cutting, and detensioning of the beam, a force transducer with amplifier tracking was employed. For proper cutting, a cutting tool specifically designed for the occasion was used, which was adaptable to elements of different widths and modular to allow measurements without removing it. A diamond-tipped angle grinder with adjustable disc width and height was used for the cutting process, with the maximum depth reaching 60mm. However, considering that the supporting tool is elevated by a total of 10mm, the actual maximum depth in the SPCE was 50mm. Finally, Figure 13

shows the different elements that facilitated the test at all times, both for measurements and functionality.

Figure 13. *Devices Used for the Test*

Two high-precision devices, DEMECs, were used to measure deformations. Two different devices were employed for this occasion, one with a measuring base of 400mm and the other with 100mm. The measurement procedure with these devices, which are highly sensitive to deformations generated in the concrete, is based on a differential measurement approach. An initial measurement, or zeroing, is performed, and then deformations that occur after making the notches are measured based on the differences. Figure 14 illustrates the measurement process.

Figure 14. *Measurements using DEMECs, Measurement base 100 and 400 MILLimeters*

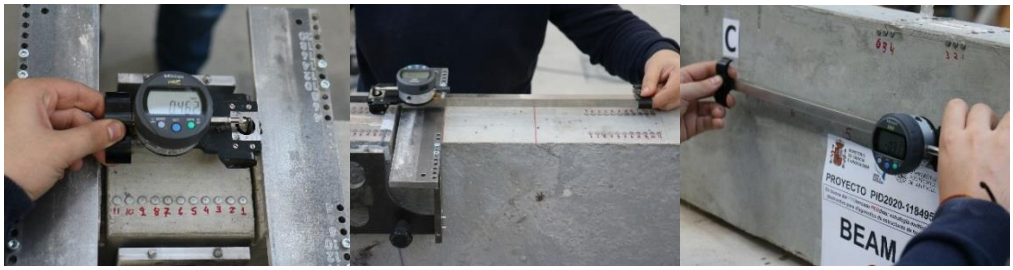

Test Sequence

The specific test presented in this article followed the following work program:

1. Placement of the beam at the test site.
2. Initial measurements taken.
3. Placement of the cable and distribution plates at the ends of the beam.
4. Installation of the force transducer and anchoring wedges for prestressing.
5. Tensioning of the prestressing cable up to 150 kN, followed by wedging of the jack (126.8 kN).

6. Once the cable force has stabilized, measurements are taken to determine the deformations after beam prestressing, accounting for losses due to wedge penetration.
7. Implementation of the cutting sequence: The execution of the test involves complete cuts of the block, which are performed based on two notches spaced 12mm apart. These notches are made in opposite directions, following the same methodology for each depth. The methodology remains consistent throughout the cutting process. After making the two notches corresponding to a complete cut, measurements are taken for all points. Initially, measurements are taken using the 400mm base DEMEC device from points RP1 to C and from C to RP2 on the top face (Z= 250mm). The purpose is to obtain deformations within the isolated block with respect to external reference points. After these measurements, measurements are taken on the lateral faces of the beams, specifically on the chord located at the center of gravity and the one located at the cable height, as well as measurement points from RP1 to C and from C to RP2 on the lateral faces. After obtaining all measurements from the 400mm base DEMEC, corresponding measurements are taken using the 100mm base DEMEC. This allows us to observe the behavior between closer points. Similarly to the 400mm base measurements, initial measurements are taken on the top face of the SPCE (Z=250mm), followed by measurements on the lateral face (Y=0). This entire sequence is performed for each of the cuts made, with depths of 5mm, 15mm, 25mm, 30mm, 35mm, 40mm, and 50mm in the concrete section.
8. After completing all the aforementioned measurements, the detensioning of the beam is carried out to allow for future tests and to evaluate the recovery capacity of the tested beam after the test.

Figure 15. *SPCE in its Final State Before Detensioning*

Numerical Model

In order to evaluate the different results, a finite element model was created using the DIANA software based on a previous study (Bauset-Tortonda et al. 2023). The model parameters were modified to capture the behavior of the beam and align it with the experimental results. Figure 16 shows the implemented model and the stress state of the prestressed concrete at the end of the test.

Figure 16. *DIANA Numerical Model*

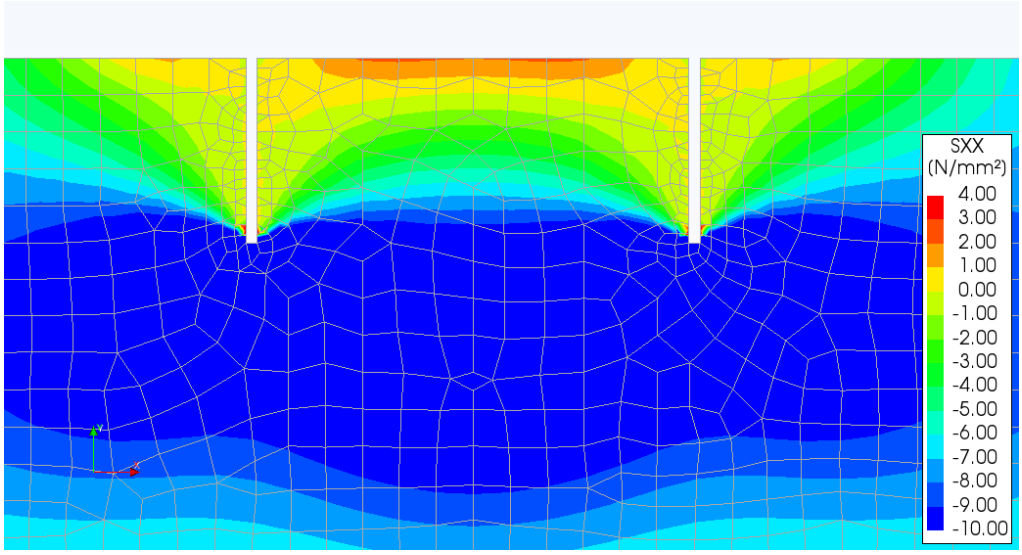

All the analysis model data were adjusted to match the tested specimen in order to verify and test the model for future studies.

Results

The following are the results obtained from the data analysis. First, the variations in displacements relative to the central point of the isolated block are shown for each of the depths at which the cuts were made, as shown in Figure 17.

Figure 17. *Average Displacement Variation in Z=250 mm*

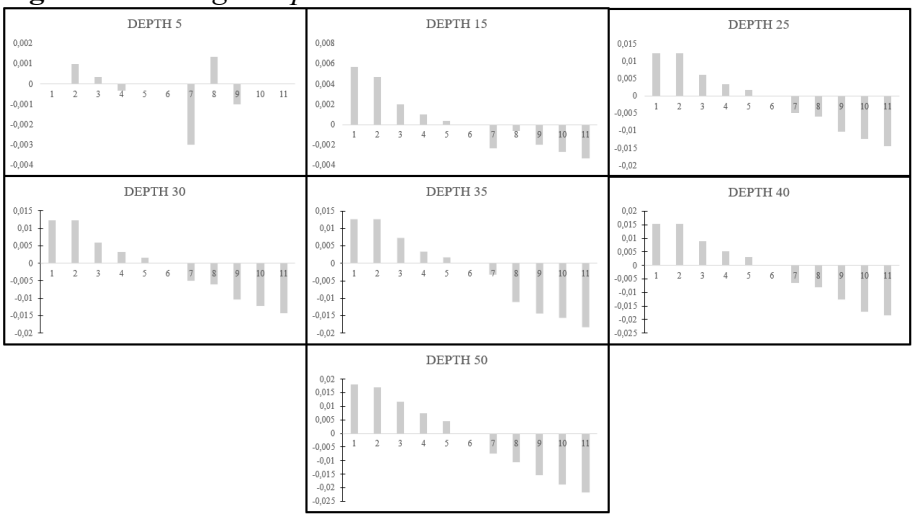

Figure 18 represents the displacement variations relative to prestressing on the lateral faces of the specimen and their evolution as the depth of the cut increases. It is important to note that measurements for points 4, 3, and 2 could not be taken due to their inoperability caused by the cutting tool. Additionally, in the 50 mm cut, references for points 12 and 11 were lost, resulting in the inability to obtain measurements for those points.

Figure 18. *Displacement Variation in Y=0 mm*

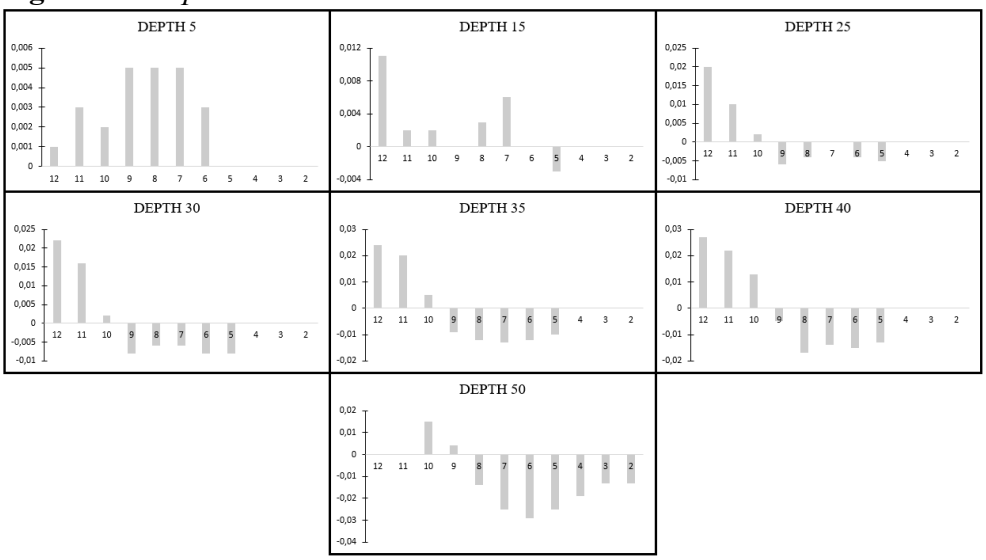

Finally, the results obtained during the experimental test are shown in Figure 19, which represents the averages of the measurements taken on the upper face (Z=250mm) from the reference point RP1 and C, as well as those from C and RP2, and the internal variation between the outermost points of the isolated block C. The graph displays the displacement variations from the prestressing operation at each of the selected depths, as well as the results obtained from the numerical modeling represented by the names Notches2D-L Ec and Notches2D-L Eci. The former uses the secant modulus, while the latter uses the tangent modulus for the corresponding elastic modulus.

Figure 19. *Representation of the Displacement Variation as a Function of the Depth of Notch*

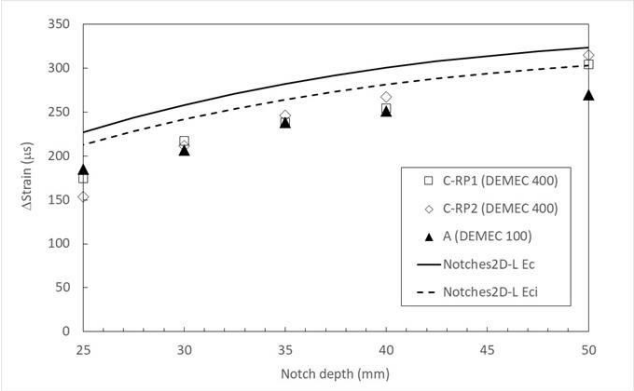

Discussion

Regarding the analysis of the results at the isolated block level, there is a significant dispersion in the results obtained for shallow depths, particularly at a depth of 5 mm. As the depth increases on the upper face (Z=250mm), there appears to be an increase in the displacement of each point as we approach the notches, indicating a complete release of stresses in those nearby points. Furthermore, as the depth increases, the variation in displacement with respect to the central point also increases, as shown in Figure 17.

Regarding the displacements obtained on the lateral faces, as observed in the figure, an upper fiber decompression occurs as the notch depth increases. This means that as the notch depth increases, the upper fibers decompress, while the immediately following fibers experience greater compression, as observed in Figure 18. However, similar to the upper face, the results obtained from the tested beam exhibit values with significant dispersion.

In relation to the values obtained for the cutting point (C) and the external reference points (RP1 and RP2), it can be observed that the displacement values obtained from the 400 mm measurement base from an external reference point and the variability between the values obtained from the internal points using the 100 mm measurement base coincide. This suggests that the reference points remain unchanged at a distance of 400 mm.

Although the values obtained from the numerical model show a similar trend in the behavior of the beam, a slight deviation is observed between the curve obtained from the experimental specimen and the numerical model. After conducting a thorough analysis, it was concluded that the elastic modulus of the concrete could be more similar to the tangent modulus than the secant modulus of the concrete. Therefore, a modification was made to the model by adjusting the modulus to correspond to the tangent modulus, as the concrete is undergoing a process of unloading. The Notches 2D-L Eci model was adjusted according to the specifications outlined in the Model Code 2010 (FIB 2010), resulting in a closer approximation to the experimental curve and improving the accuracy of the model.

Conclusions

The execution of an experimental test and the implementation of a numerical model have allowed for the study of the effect of induced notches on prestressed concrete elements. This study is essential to support the evaluation of residual prestressing force using the non-destructive and indirect methodology known as saw cutting.

From this study, the following conclusions have been drawn:

1. There is a significant dispersion in the results obtained for shallow depths, particularly at a depth of 5 mm.

2. As the depth increases on the upper face, there is an increase in the displacement of each point near the notches, indicating a complete release of stresses at those points.
3. Increasing the notch depth on the lateral faces leads to decompression of the upper fibers and increased compression in the immediately following fibers.
4. The results obtained from the tested beam exhibit values with significant dispersion on both the upper face and lateral faces.
5. The displacement values obtained from the 400 mm measurement base from an external reference point and those obtained between the internal points using the 100 mm measurement base coincide.
6. The reference points remain unchanged at a distance of 400 mm.
7. There is a slight deviation between the curve obtained from the experimental specimen and the numerical model.
8. The elastic modulus of the concrete could be more similar to the tangent modulus than the secant modulus of the concrete.
9. Adjusting the modulus to correspond to the tangent modulus in the numerical model improves accuracy and provides a closer approximation to the experimental curve.

Finally, it is important to mention that this measurement methodology reduces the influence of thermal variation caused by the temperature increase generated by saw cuts. Additionally, it would be interesting to further investigate the nonlinearity of concrete under fiber decompression circumstances in order to calibrate the model more accurately to reality and validate the model.

Acknowledgments

This work forms part of the Project “Looking for the lost prestress: multi-level strategy and non-destructive method for diagnosis of existing concrete structures” funded by the Agencia Estatal de Investigación (State Research Agency) of Spain (competitive research project PID2020-118495RB-I00 / AEI / 10.13039/501100011033 and human resources funding PRE2021-098777 / AEI / 10.13039/501100011033). The authors would also like to thank the ICITECH technical staff, Francisco J. Martorell Romero and Daniel Tasquer Val, for their valuable contributions and involvement in the development of the experimental work.

References

Azizinamini A, Keeler BJ, Rohde J, Mehrabi AB (1996) Application of a new non-destructive evaluation technique to a 25-year-old prestressed concrete girder. *PCI Journal* 41(3): 82–95.

Bauset-Tortonda I, Mateu-Sánchez JA, Serna P, Giménez-Carbó E, Castro-Bugallo MC, Martí-Vargas JR, et al. (2023) *Effect of single and twin notches in prestressed concrete beams*. Materialstoday: Proceedings.

Botte W, Vereecken E, Taerwe L, Caspeele R (2021) Assessment of posttensioned concrete beams from the 1940s: Large-scale load testing, numerical analysis and Bayesian assessment of prestressing losses. *Structural Concrete* 22(3): 1500–1522.

Calavera J (2018) *Proyecto y Cálculo de Estructuras de Hormigón*. (Project and Calculation of Concrete Structures.) Madrid: Ed. Intemac.

FIB (2010) *Fib model code for concrete structures 2010*. Bulletin no. 42. Lausanne: Fédération internationale du béton.

FIB (2016) *Partial factor methods for existing concrete structures*. Bulletin no. 80. Lausanne: Fédération internationale du béton.

Halsey JT, Miller R (1996) Destructive testing of two forty-year-old prestressed concrete bridge beams. *PCI Journal* 41(5): 84–91.

Kesavan K, Ravisankar K, Parivallal S, Sreeshylam P (2005) Technique to assess the residual prestress in prestressed concrete members. *Experimental Techniques* 29(5): 33–38.

Kim BH, Lee IK, Cho SJ (2011) Estimation of existing prestress level on bonded strand using impact-echo test. In *6th European Workshop on Structural Health Monitoring*.

Kralovanec J, Moravcík M, Jost J, (2021) Analysis of prestressing in precast prestressed concrete beams. *Civil and Environmental Engineering* 17(1): 184–191.

Kralovanec J, Bahleda F, Moravcik M, (2022a) State of prestressing analysis of 62-year-old bridge. *Materials* 15(10): 3583.

Kralovanec J, Moravčík M, Koteš P, Matejov A, (2022b) *Parametric study of saw-cut method.* In *Lecture Notes in Civil Engineering*, 10–19. Springer Science and Business Media Deutschland GmbH.

Labia Y, Saiidi MS, Douglas B (1997) Full-scale testing and analysis of 20-year-old pretensioned concrete box girders. *ACI Structural Journal* 94(5): 471–482.

Li J, Mechitov KA, Kim RE (2016) Efficient time synchronization for structural health monitoring using wireless smart sensor networks. *Structural Control Health Monitoring* 23(3): 470–486

Lynch JP (2007) An overview of wireless structural health monitoring for civil structures. *Philosophical Transactions of the Royal Society A: Mathematical, Physical and Engineering Sciences* 365(Dec): 345–372.

Naito C, Sause R, Thompson B (2008) Investigation of damaged 12-year-old pre-stressed concrete box beams. *Journal of Bridge Engineering* 13(2): 139–148.

Nawy E (2005) *Prestressed concrete: a fundamental approach*. 5th Edition. London: Pearson.

Osborn GP, Barr PJ, Petty DA, Halling MW, Brackus TR (2012) Residual prestress forces and shear capacity of salvaged prestressed concrete bridge girders. *Journal of Bridge Engineering* 17(2): 302–309.

Pape TM, Melchers RE (2013) Performance of 45-year-old corroded prestressed concrete beams. *Structures and Buildings ICE Proceedings* 166(SB10): 547–559.

Parivallal S, Ravisankar K, Nagamani K, Kesavan K (2011) Core-drilling technique for in-situ stress evaluation in concrete structures. *Experimental Techniques* 35(4): 29–34.

Pessiki S, Kaczinski M, Wescott HH (1996) Evaluation of effective prestress force in 28-year-old prestressed concrete bridge beams. *PCI Journal* 41(6): 78–89.

PIARC (2020) *Strategic plan 2020-2023*. World-Road-Association, La Défense cedex.

Riessauw FG, Taerwe L (1980) Application of a new nondestructive evaluation technique to a 25-year-old prestressed concrete girder. *PCI Journal* 25(6): 70–73.

Tabatabai H, Dickson TJ (1993) Structural evaluation of a 34-year-old precast post-tensioned concrete girder. *PCI Journal* 38(4): 50–63.

Yuan AM, Qian SL, He Y, Zhu XW (2015) Capacity evaluation of a prestressed concrete adjacent box girder with longitudinal cracks in the web. *Journal of Performance of Structural Facilities* 29(1): 04014028.